Relationship Between Alzheimer Disease–Like Pattern of ^{18}F-FDG and Fasting Plasma Glucose Levels in Cognitively Normal Volunteers

Kenji Ishibashi[1], Airin Onishi[1], Yoshinori Fujiwara[2], Kiichi Ishiwata[1], and Kenji Ishii[1]

[1]Research Team for Neuroimaging, Tokyo Metropolitan Institute of Gerontology, Tokyo, Japan; and [2]Research Team for Social Participation and Community Health, Tokyo Metropolitan Institute of Gerontology, Tokyo, Japan

Increased plasma glucose (PG) levels can alter the cerebral distribution pattern of ^{18}F-FDG uptake and reduce ^{18}F-FDG uptake, especially in the precuneus. The ^{18}F-FDG distribution pattern in cognitively normal subjects is described as an Alzheimer disease (AD)–like pattern. The aim of this study was to determine the fasting PG levels that can reduce ^{18}F-FDG uptake in the precuneus. **Methods:** Fifty-one cognitively normal volunteers (mean age ± SD, 69.7 ± 5.9 y) underwent ^{18}F-FDG PET scanning and were divided into 2 groups according to the level of fasting PG at the time of PET scanning: control (n = 31, 80 mg/dL ≤ fasting PG < 100 mg/dL) and impaired fasting glucose (IFG) (n = 20, 100 mg/dL ≤ fasting PG < 110 mg/dL). ^{18}F-FDG uptake was compared between the 2 groups using voxelwise analyses with a global normalization method and volume-of-interest (VOI)–based analyses. VOIs were placed on the precuneus, posterior cingulate, and visual cortex, and the ratio of the uptake value on the precuneus VOI to that on the visual cortex VOI (PreCne/VC ratios) and to that on the posterior cingulate VOI (PreCne/PostCin ratios) was calculated. **Results:** Whole-brain voxelwise analyses showed that ^{18}F-FDG uptake in the precuneus was significantly lower in the IFG group (P < 0.05, familywise error rate–corrected) than in the control group. VOI analyses showed significantly lower PreCne/VC ratios (P = 0.002) and PreCne/PostCin ratios (P = 0.004) in the IFG group than in the control group. **Conclusion:** The present study confirmed that increased fasting PG levels decrease ^{18}F-FDG uptake, especially in the precuneus, as in the AD-like pattern. Furthermore, the study provided initial evidence that the AD-like pattern can appear even in an individual with a mildly higher level of fasting PG (100–110 mg/dL).

Key Words: FDG; PET; precuneus, glucose; Alzheimer's disease

J Nucl Med 2015; 56:229–233
DOI: 10.2967/jnumed.114.150045

As a PET radiotracer to estimate cerebral metabolic rates of glucose utilization, ^{18}F-FDG provides information on neuronal density and function. Glucose hypometabolism is associated with reduced uptake of ^{18}F-FDG (*1*), reflecting a loss of neuronal cell number or activity. Patients with Alzheimer disease (AD) demonstrate prominently reduced uptake of ^{18}F-FDG in the precuneus and posterior cingulate regions (*2*). This characteristic distribution pattern of ^{18}F-FDG uptake is described as an AD pattern and is useful for the early diagnosis of AD.

Interestingly, in cognitively normal subjects with an increased level of plasma glucose (PG), reduced uptake of ^{18}F-FDG can be observed, especially in the precuneus, and its distribution pattern is described as an AD-like pattern (*3,4*). In addition, a recent study showed that the AD-like pattern during a hyperglycemic state is reversible and independent of amyloid-β (Aβ) deposition or apolipoprotein E ε4 genotype (*5*). These studies indicate that an individual with higher PG levels can be erroneously diagnosed with AD using ^{18}F-FDG and PET due to reduced uptake of ^{18}F-FDG in the precuneus.

Guidelines for ^{18}F-FDG PET brain imaging usually recommend rescheduling the scanning if the PG level is greater than approximately 150 mg/dL (*6*), as increased PG levels reduce cerebral uptake of ^{18}F-FDG (*7–10*) because of competition with glucose for both transport and metabolism and because of an increase in stochastic noise (*11*). According to previous studies (*3,4*), however, PG levels of less than 130 mg/dL can reduce ^{18}F-FDG uptake in the precuneus and can alter the cerebral distribution pattern of ^{18}F-FDG from normal to AD-like.

The goal of this study was to determine the fasting PG levels that can reduce ^{18}F-FDG uptake in the precuneus, to avoid erroneous diagnosis of AD. For this purpose, we performed ^{18}F-FDG PET scanning on cognitively normal volunteers with fasting PG levels of 80–110 mg/dL. We also discuss the link between increased fasting PG levels and the AD-like pattern in the precuneus.

MATERIALS AND METHODS

Research Participants

The Ethics Committee of the Tokyo Metropolitan Institute of Gerontology approved the study protocol, and written informed consent was obtained from all participants. The participants comprised 51 cognitively normal volunteers (3 men and 48 women; age range, 57–83 y [mean age ± SD, 69.7 ± 5.9 y]) and 15 patients with AD (5 men and 10 women; age range, 50–83 y [mean age, 67.4 ± 9.7 y]) who were diagnosed on the basis of clinical criteria (*12*) and positive findings on Aβ PET imaging using ^{11}C-Pittsburgh compound B. Volunteers were excluded if their Mini-Mental State Examination score was less than 27, if their body mass index was less than 18.5 or more than 25.0, if they met the criteria for mild cognitive impairment (*13*), or if they had a history of diabetes. Volunteers with a neurologic condition or any other uncontrolled health condition were also excluded. PET data from 15 patients with AD were from a database for PET studies at the Tokyo Metropolitan Institute of Gerontology.

Received Oct. 14, 2014; revision accepted Dec. 11, 2014.
For correspondence or reprints contact: Kenji Ishibashi, Research Team for Neuroimaging, Tokyo Metropolitan Institute of Gerontology, 35-2 Sakae-cho, Itabashi-ku, Tokyo 173-0015, Japan.
E-mail: ishibashi@pet.tmig.or.jp
Published online Jan. 8, 2015.

The 51 cognitively normal volunteers were divided into 2 groups according to their fasting PG levels at the time of ^{18}F-FDG PET scanning: control (n = 31, 80 mg/dL ≤ fasting PG < 100 mg/dL) and impaired fasting glucose (IFG) (n = 20, 100 mg/dL ≤ fasting PG < 110 mg/dL). The sample data are summarized in Table 1.

PG Measurement and PET Scanning

After more than 5 h of fasting, each participant underwent ^{18}F-FDG PET scanning at the Tokyo Metropolitan Institute of Gerontology for research purposes. Fasting PG levels were measured twice at the time of PET scanning using a medical device (Caresist; Horiba, Ltd.), and the 2 values were averaged. The measurement system for PG was based on the enzyme electrode method, which integrates a hydrogen peroxide electrode with a glucose oxidase immobilized membrane.

PET scanning was performed on a SET-2400W scanner (Shimadzu, Ltd.) in 3-dimensional mode. Images from 50 slices were obtained with a 2.054 × 2.054 × 3.125 mm voxel size and a 128 × 128 matrix size. Transmission data were acquired using a rotating ^{68}Ga/^{68}Ge rod source for measured attenuation correction. Static emission data were acquired for 45–51 min after an intravenous bolus injection of 150 MBq of ^{18}F-FDG. Data were reconstructed after correction for decay, attenuation, and scatter.

PET Image Processing and Data Analysis

All participants underwent MR scanning. The images were processed using the FMRIB Software Library, version 5.0.4 (FSL; Oxford University) and were used for the subsequent PET image processing. The static ^{18}F-FDG images were coregistered to the corresponding structural MR images using FSL FLIRT. The coregistered images of ^{18}F-FDG were then warped into Montreal Neurological Institute (MNI) space using MR imaging–guided spatial normalization (FSL FNIRT). On the warped ^{18}F-FDG images in MNI space, voxelwise analyses and volume-of-interest (VOI)–based analyses were performed.

Data Analysis and Statistical Analysis

First, whole-brain voxelwise analyses were performed. The warped ^{18}F-FDG images in MNI space were smoothed with a gaussian kernel of σ 8 mm to improve the signal-to-noise ratio and were proportionally scaled to a global mean value. The normalized images representing ^{18}F-FDG uptake were finally completed. Using Statistical Parametric Mapping, version 8 (SPM8; Wellcome Trust Center for Neuroscience), implemented in MATLAB, version R2014a (The MathWorks), a 2-sample t test was performed to detect the voxels in which ^{18}F-FDG uptake decreased, compared with the control group. Statistical t maps of "control group: 1 and test group: −1" contrast were calculated using a height threshold of $P < 0.05$, familywise error rate–corrected, excluding clusters smaller than 50 voxels. The SPM t maps were then transformed to the P maps.

VOI-based analyses were then performed to assess the changes in the distribution pattern of ^{18}F-FDG and to corroborate the results of voxelwise analyses. VOIs were placed on the precuneus and posterior cingulate regions for which voxelwise analyses found statistical significance and on the visual (intracalcarine) cortex as a reference region because ^{18}F-FDG uptake in the visual cortex is relatively preserved even in advanced stages of AD (*14*). A visual cortex VOI was selected from the Harvard–Oxford atlas (included in FSL). Precuneus and posterior cingulate VOIs were drawn in MNI space and were located within the precuneus and posterior cingulate regions, respectively, which are spatially defined in the Harvard–Oxford atlas. The VOIs were moved onto the warped ^{18}F-FDG images in MNI space, and the uptake values on the VOIs were extracted. Then, the ratio of the uptake value on the precuneus VOI to that on the visual cortex VOI (PreCne/VC ratios) and to that on the posterior cingulate VOI (PreCne/PostCin ratios) was calculated. PreCne/VC ratios represent normalized ^{18}F-FDG uptake, as the visual cortex was set as a reference region. PreCne/PostCin ratios indicate the change in the distribution pattern of ^{18}F-FDG in the precuneus and posterior cingulate regions. The differences in the ratios between the 2 groups were tested using the independent t test. Statistical significance was set at a P value of less than 0.05 (2-tailed).

TABLE 1
Participant Characteristics

Group	Control (n = 31)	IFG (n = 20)	AD (n = 15)
Age			
Range	57–83	63–82	50–83
Mean	68.1	72.2	67.4
SD	6.2	4.6	9.7
Fasting glucose level			
Minimum	80.0	101.0	82.5
Maximum	98.5	108.5	99.5
Mean	89.0	103.9	92.5
SD	5.60	2.21	5.09

RESULTS

Whole-Brain Voxelwise Analyses

Figure 1B highlights the precuneus and posterior cingulate regions in which prominently reduced uptake of ^{18}F-FDG was observed in the AD group, compared with the control group, as in the typical AD pattern. For the cognitively normal volunteers, whole-brain SPM analyses revealed one cluster located mainly in the precuneus region at $P < 0.05$, familywise error rate–corrected (Fig. 1A). MNI coordinates of the peak-level voxel in Figures 1A and 1B were located in the precuneus.

VOI-Based Analyses

Figure 2A shows significantly lower PreCne/VC ratios in the IFG group than in the control group ($P = 0.002$) and prominently lower PreCne/VC ratios in the AD group than in the IFG group ($P < 0.001$). Figure 2B shows significantly lower PreCne/PostCin ratios in the IFG group than in the control group ($P = 0.004$); however, the ratios were not statistically significant between the IFG and AD groups ($P = 0.96$).

The ^{18}F-FDG images normalized using the uptake values from the visual cortex VOI and from the posterior cingulate VOI were averaged in MNI space and are displayed in Figures 3C–3E (middle row) and Figures 3F–3H (bottom row), respectively. The visual inspection of Figures 3C–3E and Figures 3F–3H was consistent with that of Figures 2A and 2B, respectively. When normalized to the value from the visual cortex VOI (visual cortex = 1), ^{18}F-FDG uptake in the precuneus visibly decreased in the IFG group (Fig. 3D) and was depleted in the AD group (Fig. 3E), compared with the control group (Fig. 3C). When normalized to the value from the posterior cingulate VOI (posterior cingulate = 1), it was possible to distinguish ^{18}F-FDG uptake in the precuneus between the control and IFG groups (Figs. 3F and 3G).

DISCUSSION

Increased PG levels in both fasting and glucose-loading conditions reduce ^{18}F-FDG uptake, especially in the precuneus,

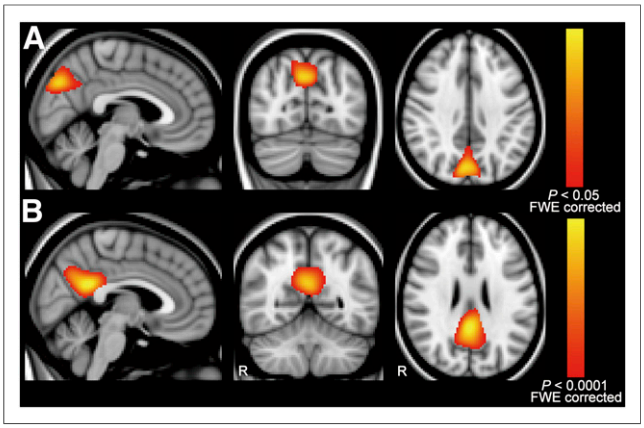

FIGURE 1. Results of whole-brain voxelwise analyses. Significant clusters by 2-sample *t* test, using "control group (n = 31): 1 and test group: −1" contrast, are displayed on MNI standard brain with MNI coordinates of peak-level voxel in sagittal, coronal, and axial sections. For IFG group (A), height threshold was set at $P < 0.05$, familywise error rate–corrected (T value > 4.45). For AD group (B), it was set at $P < 0.0001$, familywise error rate–corrected (T value > 6.54), to illustrate prominent hypoglycemic regions as typical AD pattern. MNI coordinates (*x, y, z* mm) for A and B were (4, −74, 36) and (4, −56, 26), respectively, and were located in precuneus. Yellow–red scales represent magnitude of *P* values. FWE = familywise error rate.

and can alter the cerebral distribution pattern of ^{18}F-FDG uptake from a normal pattern to the AD-like pattern in cognitively normal subjects (*3,4*). In an ^{18}F-FDG PET study of 9 healthy older subjects, glucose loading yielded a reduction of ^{18}F-FDG uptake in AD-related cortical regions (*3*). In a cross-sectional study of 124 cognitively normal older subjects, higher fasting PG levels were significantly correlated with the magnitude of reduced uptake of ^{18}F-FDG in AD-related cortical regions (*4*). We recently reported a case of a 70-y-old patient with mild cognitive impairment and showed that reduced uptake of ^{18}F-FDG in the precuneus during the glucose-loading condition was reversible and independent of Aβ deposition and apolipoprotein E ε4 genotype (*5*). The current study confirmed those previous findings and additionally provided initial evidence that ^{18}F-FDG uptake in the precuneus decreases even at mildly higher levels of fasting PG (100 mg/dL ≤ fasting PG < 110 mg/dL).

Figure 1A may imply that the significant cluster does not include the lower part of the precuneus and posterior cingulate, which are the center of the AD pattern as shown in Figure 1B. When, however, the height threshold of *P* value was set at a more liberal level, the cluster shown in Figure 1A extended to these areas and overlapped with the significant cluster shown in Figure 1B. Additionally, VOI-based analyses showed that both PreCne/VC and PreCne/PosCin ratios in the IFG group decreased toward the levels in the AD group (Fig. 2). These voxelwise and VOI-based analyses indicate that the change in the distribution pattern of ^{18}F-FDG, especially in the precuneus, leads to the appearance of the AD-like pattern, and this pattern can appear in an individual with a fasting PG of 100 mg/dL or more. Thus, statistical voxelwise analyses may detect an individual with a fasting PG level of 100 mg/dL or more as AD if the control group is composed of subjects with a fasting PG level of less than 100 mg/dL. By visual inspection, the difference in the distribution pattern of ^{18}F-FDG is small between the control and IFG groups (Fig. 3). However, when the levels of fasting PG increase, the difference can be large and easily detected by visual inspection (*5*). Therefore, to avoid erroneous diagnosis of AD, it is essential to understand the distribution pattern of ^{18}F-FDG in the context of an individual's fasting PG levels. When statistical analyses are performed to assess ^{18}F-FDG uptake, fasting PG levels should be matched between groups.

Increased insulin levels are usually observed with increased fasting PG levels (*15,16*) and play an important role in modulating neuronal activity since insulin affects glucose utilization in the central nervous system (*17,18*). Increased fasting PG and insulin levels are associated with greater insulin resistance (*19*). In cognitively normal patients with prediabetes or early type 2 diabetes, greater insulin resistance decreases uptake of ^{18}F-FDG in the precuneus region (*20,21*). Therefore, a set of increased fasting PG and insulin levels is considered to cause reduced uptake of ^{18}F-FDG (i.e., glucose hypometabolism) in the precuneus. The default mode network (DMN) may be an important key to understanding the link between increased fasting PG and insulin levels and glucose hypometabolism in the precuneus. The DMN is characterized by high activity when the mind is not engaged in specific behavioral tasks and low activity during focused attention on the external environment, and the precuneus is its posterior component (*22*). The precuneus comprises the functional core of the DMN and plays an important role in regulating complex cognition and behavior (*23–25*). The functional connectivity in the DMN, including the precuneus, decreases in cognitively normal patients with type 2 diabetes, and the magnitude of the reduced connectivity is associated with insulin resistance (*26*). These lines of evidence, combined with our current observations, support an explanation that increased fasting PG and insulin levels (i.e., greater insulin resistance) causes a reduction of functional connectivity in the DMN, leading to reduced uptake of ^{18}F-FDG (i.e., glucose hypometabolism), especially in the precuneus. Furthermore, prolonged stress can affect the pattern of activity in the DMN (*27*). As an alternative explanation, increased fasting PG levels may act as a stress test to unmask a very early neurodegenerative disorder that affects the DMN.

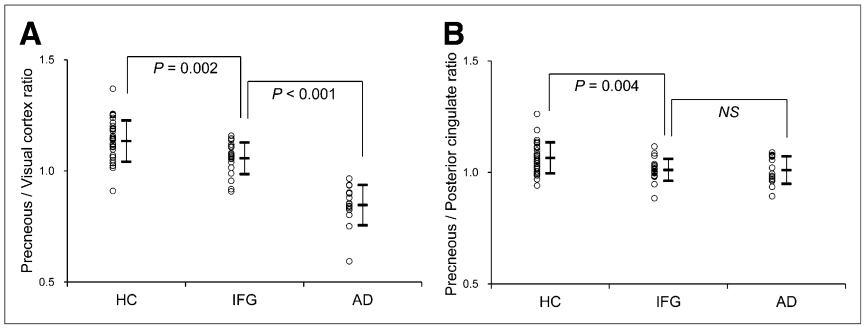

FIGURE 2. Precuneus/visual cortex and precuneus/posterior cingulate ratios. Ratios of precuneus/visual cortex (A) and precuneus/posterior cingulate (B) were compared between HC, IFG, and AD groups. Vertical bars represent mean ± SD. HC = healthy control; NS = not significant.

The precuneus is also pivotal for the pathophysiology of AD. Glucose hypometabolism in the precuneus is a hallmark of the diagnosis of early AD (*2,28*), and this region is vulnerable to Aβ deposition (*29*). Functional connectivity in the DMN is also

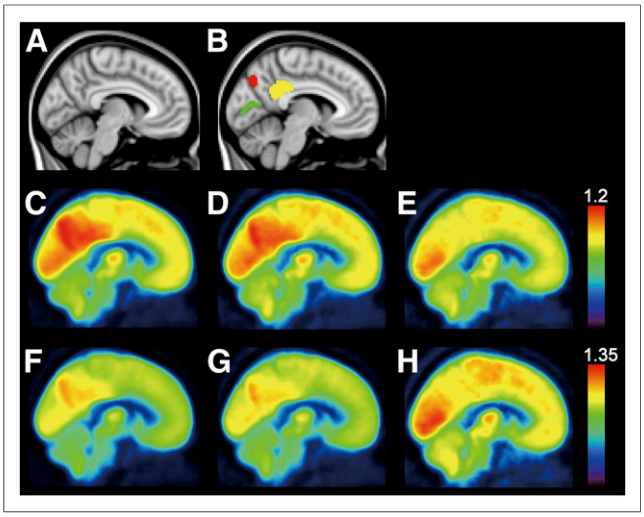

FIGURE 3. VOIs and normalized ^{18}F-FDG images in control, IFG, and AD groups. (A) MNI standard brain is displayed in sagittal section as anatomic reference for VOIs and ^{18}F-FDG images. MNI coordinate was x = 4 mm. (B) VOIs placed on precuneus (red), posterior cingulate (yellow), and visual cortex (green) are displayed. VOI volumes are 535 voxels, 1,000 voxels, and 432 voxels for precuneus, posterior cingulate, and visual cortex, respectively. (C–E) ^{18}F-FDG images in control group (C), IFG group (D), AD group (E) were normalized using values of ^{18}F-FDG uptake in visual cortex and were averaged in MNI space. Rainbow scale represents values of ^{18}F-FDG uptake (visual cortex = 1). (F–H) ^{18}F-FDG images in control group (F), IFG group (G), and AD group (H) were normalized using values of ^{18}F-FDG uptake in posterior cingulate and were averaged in MNI space. Rainbow scale represents values of ^{18}F-FDG uptake (posterior cingulate = 1).

impaired in patients with AD and asymptomatic older individuals with Aβ accumulation (*30*). A recent cross-sectional study of 207 cognitively normal older adults found that decreased cerebrospinal fluid Aβ was associated with a reduction of functional connectivity in the DMN (*31*). Furthermore, it suggested that Aβ pathology affects the DMN integrity before clinical onset of AD and that impairment of the DMN is associated with current and future cognitive decline (*31*). On the other hand, type 2 diabetes is a risk factor for AD (*32–34*), although the pathophysiologic mechanism between diabetes and AD is unknown. However, as an extension of this study, impairment of the DMN may represent a link between type 2 diabetes and AD.

According to the criteria for diabetes (*35*), fasting PG levels of <100 mg/dL, ≥100 and <126 mg/dL, and ≥126 mg/dL are defined as normal, IFG, and diabetes, respectively (*35*). This classification is based largely on the following evidence: the risk of having or developing retinopathy increases at fasting PG levels above 126 mg/dL, the risk of diabetes increases markedly at fasting PG levels above approximately 100 mg/dL, and setting the cutoff level of fasting PG at approximately 100 mg/dL optimizes the sensitivity and specificity for predicting future diabetes (*36–38*). On the other hand, higher fasting PG levels are known to be associated with cognitive decline as measured by a battery of neuropsychological tests (*39,40*), indicating the existence of some threshold level of fasting PG for cognitive decline. On the basis of the classification of fasting PG levels by these criteria (*35*) and our findings, the threshold levels of fasting PG for the onset of cognitive decline may be about 100 mg/dL, although further studies are necessary to elucidate this issue.

One of the limitations of the present study is the absence of Aβ PET imaging in the cognitively normal volunteers. As increasing PG level is a risk factor for AD (*34*), some of the subjects in the IFG group may already be at a stage of preclinical AD. Future studies investigating this issue are needed to confirm the results of the present study.

CONCLUSION

The present study confirms that increased fasting PG levels decrease ^{18}F-FDG uptake, especially in the precuneus, and its distribution pattern is similar to the AD pattern. The study also provides initial evidence that the AD-like pattern can appear even in an individual with mildly higher levels of fasting PG (100–110 mg/dL). To avoid an erroneous diagnosis of AD, it is essential to understand the distribution pattern of ^{18}F-FDG corresponding to the fasting PG levels.

DISCLOSURE

The costs of publication of this article were defrayed in part by the payment of page charges. Therefore, and solely to indicate this fact, this article is hereby marked "advertisement" in accordance with 18 USC section 1734. This work was supported in part by the Nakayama Foundation for Human Science. No other potential conflict of interest relevant to this article was reported.

ACKNOWLEDGMENTS

We thank Hatsumi Endo, Hiroko Tsukinari, and Kunpei Hayashi for their technical assistance.

REFERENCES

1. Suhonen-Polvi H, Ruotsalainen U, Kinnala A, et al. FDG-PET in early infancy: simplified quantification methods to measure cerebral glucose utilization. *J Nucl Med.* 1995;36:1249–1254.
2. Sperling RA, Aisen PS, Beckett LA, et al. Toward defining the preclinical stages of Alzheimer's disease: recommendations from the National Institute on Aging-Alzheimer's Association workgroups on diagnostic guidelines for Alzheimer's disease. *Alzheimers Dement.* 2011;7:280–292.
3. Kawasaki K, Ishii K, Saito Y, Oda K, Kimura Y, Ishiwata K. Influence of mild hyperglycemia on cerebral FDG distribution patterns calculated by statistical parametric mapping. *Ann Nucl Med.* 2008;22:191–200.
4. Burns CM, Chen K, Kaszniak AW, et al. Higher serum glucose levels are associated with cerebral hypometabolism in Alzheimer regions. *Neurology.* 2013;80:1557–1564.
5. Ishibashi K, Miura Y, Oda K, Ishiwata K, Ishii K. Alzheimer's disease-like pattern of ^{18}F-FDG uptake during a hyperglycemic state and negative ^{11}C-PiB binding in a patient with mild cognitive impairment. *J Alzheimers Dis.* 2014;42:385–389.
6. Varrone A, Asenbaum S, Vander Borght T, et al. EANM procedure guidelines for PET brain imaging using [^{18}F]FDG, version 2. *Eur J Nucl Med Mol Imaging.* 2009;36:2103–2110.
7. Wahl RL, Henry CA, Ethier SP. Serum glucose: effects on tumor and normal tissue accumulation of 2-[F-18]-fluoro-2-deoxy-D-glucose in rodents with mammary carcinoma. *Radiology.* 1992;183:643–647.
8. Hara T, Higashi T, Nakamoto Y, et al. Significance of chronic marked hyperglycemia on FDG-PET: is it really problematic for clinical oncologic imaging? *Ann Nucl Med.* 2009;23:657–669.
9. Yamada K, Endo S, Fukuda H, et al. Experimental studies on myocardial glucose metabolism of rats with ^{18}F-2-fluoro-2-deoxy-D-glucose. *Eur J Nucl Med.* 1985;10:341–345.
10. Márián T, Balkay L, Fekete I, et al. Hypoglycemia activates compensatory mechanism of glucose metabolism of brain. *Acta Biol Hung.* 2001;52:35–45.
11. Wienhard K. Measurement of glucose consumption using [^{18}F]fluorodeoxyglucose. *Methods.* 2002;27:218–225.
12. McKhann GM, Knopman DS, Chertkow H, et al. The diagnosis of dementia due to Alzheimer's disease: recommendations from the National Institute on Aging-Alzheimer's Association workgroups on diagnostic guidelines for Alzheimer's disease. *Alzheimers Dement.* 2011;7:263–269.

13. Albert MS, DeKosky ST, Dickson D, et al. The diagnosis of mild cognitive impairment due to Alzheimer's disease: recommendations from the National Institute on Aging-Alzheimer's Association workgroups on diagnostic guidelines for Alzheimer's disease. *Alzheimers Dement.* 2011;7:270–279.
14. Ishii K. Clinical application of positron emission tomography for diagnosis of dementia. *Ann Nucl Med.* 2002;16:515–525.
15. Cambien F, Warnet JM, Eschwege E, Jacqueson A, Richard JL, Rosselin G. Body mass, blood pressure, glucose, and lipids: does plasma insulin explain their relationships? *Arteriosclerosis.* 1987;7:197–202.
16. Chen CH, Tsai ST, Chou P. Correlation of fasting serum C-peptide and insulin with markers of metabolic syndrome-X in a homogenous Chinese population with normal glucose tolerance. *Int J Cardiol.* 1999;68:179–186.
17. Grillo CA, Piroli GG, Hendry RM, Reagan LP. Insulin-stimulated translocation of GLUT4 to the plasma membrane in rat hippocampus is PI3-kinase dependent. *Brain Res.* 2009;1296:35–45.
18. Lucignani G, Namba H, Nehlig A, Porrino LJ, Kennedy C, Sokoloff L. Effects of insulin on local cerebral glucose utilization in the rat. *J Cereb Blood Flow Metab.* 1987;7:309–314.
19. Wallace TM, Levy JC, Matthews DR. Use and abuse of HOMA modeling. *Diabetes Care.* 2004;27:1487–1495.
20. Baker LD, Cross DJ, Minoshima S, Belongia D, Watson GS, Craft S. Insulin resistance and Alzheimer-like reductions in regional cerebral glucose metabolism for cognitively normal adults with prediabetes or early type 2 diabetes. *Arch Neurol.* 2011;68:51–57.
21. Gandhe MB, M L, Srinivasan AR. Evaluation of body mass index (BMI) percentile cut-off levels with reference to insulin resistance: a comparative study on south Indian obese and non-obese adolescents. *J Clin Diagn Res.* 2013;7:1579–1582.
22. Anticevic A, Cole MW, Murray JD, Corlett PR, Wang XJ, Krystal JH. The role of default network deactivation in cognition and disease. *Trends Cogn Sci.* 2012;16:584–592.
23. Fransson P, Marrelec G. The precuneus/posterior cingulate cortex plays a pivotal role in the default mode network: evidence from a partial correlation network analysis. *Neuroimage.* 2008;42:1178–1184.
24. Utevsky AV, Smith DV, Huettel SA. Precuneus is a functional core of the default-mode network. *J Neurosci.* 2014;34:932–940.
25. Cavanna AE, Trimble MR. The precuneus: a review of its functional anatomy and behavioural correlates. *Brain.* 2006;129:564–583.
26. Musen G, Jacobson AM, Bolo NR, et al. Resting-state brain functional connectivity is altered in type 2 diabetes. *Diabetes.* 2012;61:2375–2379.
27. Soares JM, Sampaio A, Ferreira LM, et al. Stress impact on resting state brain networks. *PLoS ONE.* 2013;8:e66500.
28. Friedland RP, Budinger TF, Ganz E, et al. Regional cerebral metabolic alterations in dementia of the Alzheimer type: positron emission tomography with [^{18}F]fluorodeoxyglucose. *J Comput Assist Tomogr.* 1983;7:590–598.
29. Klunk WE, Engler H, Nordberg A, et al. Imaging brain amyloid in Alzheimer's disease with Pittsburgh compound-B. *Ann Neurol.* 2004;55:306–319.
30. Sperling RA, Laviolette PS, O'Keefe K, et al. Amyloid deposition is associated with impaired default network function in older persons without dementia. *Neuron.* 2009;63:178–188.
31. Wang L, Brier MR, Snyder AZ, et al. Cerebrospinal fluid Abeta42, phosphorylated Tau181, and resting-state functional connectivity. *JAMA Neurol.* 2013;70:1242–1248.
32. Craft S. Insulin resistance and Alzheimer's disease pathogenesis: potential mechanisms and implications for treatment. *Curr Alzheimer Res.* 2007;4:147–152.
33. Luchsinger JA. Type 2 diabetes and cognitive impairment: linking mechanisms. *J Alzheimers Dis.* 2012;30(suppl 2):S185–S198.
34. Xu W, Qiu C, Winblad B, Fratiglioni L. The effect of borderline diabetes on the risk of dementia and Alzheimer's disease. *Diabetes.* 2007;56:211–216.
35. American-Diabetes-Association. Diagnosis and classification of diabetes mellitus. *Diabetes Care.* 2005;28(suppl 1):S37–S42.
36. Genuth S, Alberti KG, Bennett P, et al. Follow-up report on the diagnosis of diabetes mellitus. *Diabetes Care.* 2003;26:3160–3167.
37. Gabir MM, Hanson RL, Dabelea D, et al. The 1997 American Diabetes Association and 1999 World Health Organization criteria for hyperglycemia in the diagnosis and prediction of diabetes. *Diabetes Care.* 2000;23:1108–1112.
38. Report of the Expert Committee on the Diagnosis and Classification of Diabetes Mellitus. *Diabetes Care.* 1997;20:1183–1197.
39. Di Bonito P, Di Fraia L, Di Gennaro L, et al. Impact of impaired fasting glucose and other metabolic factors on cognitive function in elderly people. *Nutr Metab Cardiovasc Dis.* 2007;17:203–208.
40. Yaffe K, Blackwell T, Kanaya AM, Davidowitz N, Barrett-Connor E, Krueger K. Diabetes, impaired fasting glucose, and development of cognitive impairment in older women. *Neurology.* 2004;63:658–663.